Journal of the National Academy of Forensic Engineers®

http://www.nafe.org

ISSN: 2379-3252

DOI: 10.51501/jotnafe.v38i2

Vol. 38 No. 2 December 2021

Forensic Engineering Analysis of a Crash Caused by Swingout of an Articulated Booster on a Semi-Trailer

By Shawn Ray, PE (NAFE 970S), Donald J. Fournier, Jr., PE (NAFE 626S), Reza Vaghar, PhD, PE (NAFE 979S), and Steven Mitchell, PhD, PE

Abstract

An unloaded lowboy trailer with an articulated booster axle was traversing a curved exit ramp when the trailer tires lost traction, and the booster axle redirected the rear of the trailer into oncoming traffic. The reconstruction used a detailed analysis of roadway geometry, truck geometry, and suspension characteristics to determine the cause of the trailer swingout. A comprehensive topographical map was created from 3D laser scans. The interaction of each tire with the pavement surface was used to determine the individual wheel loads. Dynamic analysis of the curved path quantified the speed required to cause loss of traction and subsequent swingout.

Keywords

Truck-tractor, lowboy semi-trailer, swingout, booster axle, dolly, rolling lateral friction, cross over collision, forensic engineering

Background

In early afternoon in February, a truck-tractor towing an empty lowboy semi-trailer with a booster axle was exiting a major turnpike proceeding toward the highway on a bi-directional entrance-exit ramp with a single lane in each direction when the truck's trailer drifted into the opposing lane of traffic. Meanwhile, a pickup on the same ramp approached from the opposite direction and collided with the rear of the trailer. After the first collision, a passenger car collided with the rear of the pickup, which had stopped abruptly due to the collision with the trailer.

Witnesses described the rear of the lowboy trailer as having rapidly rotated across the centerline median, swinging into the oncoming lane. Later, it was determined that the rear tires of the trailer lost traction, causing the trailer to drift clockwise into the opposing lane, colliding with the pickup. The road surface was wet due to light rain. It was daylight but overcast, and the ramp advisory posted speed was 35 mph.

Motivation

The truck-tractor and empty lowboy semi-trailer were on the inside of the curve, and a pickup, car, and other traffic were on the outside of the curve. Traffic was moderately heavy, and witnesses were consistent in their description. No pre-impact physical evidence, such as tire marks, was documented. The witnesses, area of impact, and reconstruction indicated that the rear of the semi-trailer suddenly swung into the outside of the curved path (crossing over the centerline) before colliding with the oncoming pickup.

The initial task was to collect evidence, orient the vehicles at impact and final rest, and determine how the collision occurred. Then stepping back in time to the moments just prior to collision, the positions of the vehicle were plotted on scaled diagrams.

Based on site evidence and witness statements, the rear of the trailer suddenly departed the curved path of the tractor-trailer and crossed over the centerline median without warning to its driver. The quick lateral movement without any tire marks indicated the articulated booster axle was causing the redirection of the rear of the trailer. The empty lowboy semi-trailer was longer than most truck-tractor-trailer combinations so that it could carry large, heavy cargo.

The theory was proposed that the length of the trailer and the articulated booster axle enabled a bridging effect

Shawn Ray, PE, 5410 NW 33rd, Suite 100, Fort Lauderdale, FL 33309, (954) 777 4790, shawnray1@gmail.com
DOI: 10.51501/jotnafe.v38i2.125

on the compound roadway curves that caused the articulated booster axle to lift the rear wheels of the trailer. This loss of normal force reduced the lateral tire friction, which created an instability. This, in turn, caused the articulated booster axle and the rear of the trailer to follow a line tangent to the curve rather than the intended roadway curve.

The next phase of the collision reconstruction was to evaluate this theory and to determine if the theory was consistent with the evidence.

Due to the specific set of circumstances and the bridging effect created by the long truck-trailer combination on this ramp, traditional planar accident reconstruction techniques and crash simulation software proved insufficient to reconstruct the incident. Advanced three-dimensional (3D) graphics and geometric techniques (together with specific physics-based kinematic equations) were used to reconstruct this accident and explain the unusual combination of factors that led to the loss of traction at the rear of the trailer.

The accident investigation included a detailed analysis of the physical evidence, roadway geometry, truck geometry, and suspension effects using high-definition (HD) 3D laser scanning, electronic total station survey data, and unmanned aerial vehicle (UAV) aerial imagery.

The reconstruction included a customized kinematic model of the truck-tractor, semi-trailer, and booster axle, which was created by the authors to evaluate the vehicle-specific dynamics. Multiple graphics and scale models were used to demonstrate the findings of the accident reconstruction and illustrate the specific combination of truck-trailer and roadway factors that led to this event.

Forensic Engineering Analysis and Collision Evaluation

The collision evaluation included a review of the following material:

1. Police traffic crash report and police investigation material.

2. Scene photographs.

3. Witness statements and depositions.

4. Service records for the tractor trailer, vehicle specifications, records, and history for each vehicle.

The investigation tasks included:

1. Documenting the site with photographs and video at ground level and from the air.

2. Documenting the path and speed of traffic with aerial video.

3. Documenting the roadway with HD 3D laser scans and electronic total station measurements.

4. Examining, photographing, and measuring the truck and trailer.

5. Documenting the truck and trailer with HD 3D laser scans.

6. Inspecting the brakes of the truck and trailer.

7. Conducting an axle-by-axle measurement of weight with varying booster axle pressures.

8. Imaging the crash data from the pickup's Airbag Control Module (ACM).

9. Performing drag factor tests at the site and similar surfaces in the surrounding area with a towed full-size trailer tire.

Accident Site

The accident site was a two-lane, bi-directional entrance-exit ramp with one lane of traffic in each direction. The opposing lanes were separated by a small, raised median and solid yellow painted centerlines approximately 1 foot from the centerline median curb. **Figure 1** shows

Figure 1
Accident site location and roadway configuration.

an aerial photograph of the accident site. For orientation purposes, north is to the bottom of the figure; the turnpike is the north-south highway on the left of the figure.

The ramp interchange was originally constructed between 1963 and 1967 as part of the turnpike and state route construction projects. Multiple overlays and maintenance projects have occurred during the 50-plus-year life of the roadway. Changes to the surface included reduction in the elevation difference between the road surface and the center raised median curb and surface slopes — it was not in compliance with current roadway standards[1]. This ramp has since been reconstructed to bring it up to current standards as part of a previously planned construction project.

The ramp was comprised of two 15-foot lanes with paved shoulders on the outside of each side. The roadway combined three changing geometries simultaneously: a horizontal curve, a vertical curve, and superelevation.

A detailed set of 3D scans and total station measurements (in combination with aerial drone photography) were used to document the accident site, roadway geometry, alignment, superelevation, and pavement elevations. These characteristics were then analyzed as part of a detailed reconstruction.

In the area of the collision, there was a 2-foot paved shoulder along the outside radius for southbound traffic and a 5-foot shoulder along the inside radius for northbound traffic. In the area of the collision, the radius of the center of the median was 250 feet. Vehicles heading along the inside lane (in a northerly direction) were proceeding downhill; vehicles in the outside lane (in a southerly direction) were proceeding uphill. The downhill slope in the area of the collision decreased from 4.5% to 1% as vehicles proceeded down the ramp.

There was a superelevation associated with the curve that increased from 8% to 12%. Along the ramp, each of the variables (radius, grade, and superelevation) changed with respect to location — and the rate of change was not constant. **Figure 2** shows the tractor driver's approach to the area of the cross-over event.

Traffic was described as moderate-to-heavy, and witnesses each reported traveling at or slightly below the advisory speed of 35 mph. **Figure 3** shows the post-impact locations and condition of the pickup.

Figure 2
Truck driver view approaching the area of the crash event.

Figure 3
Collision scene photo taken by investigating officer.

The pickup was in the outside lane on an uphill grade. The truck was heading downhill in the inside lane.

The interrelationship between the changing roadway geometry and the truck/trailer dimensions created a bridge, lifting the trailer tires as the truck entered the bowl created by the geometry of the exit ramp. The trailer weight was transferred to the articulated booster axle, which steered along a constant elevation curved path nearly tangent to the roadway centerline median.

Truck-Tractor and Semi-Trailer

The first vehicle was a 2007 Class 8 conventional cab 6x4 tractor chassis. The engine's event data recorder was set with the "Quick Stop" record "off" consistent with the factory default position and did not record sudden deceleration data. The tractor was pulling a lowboy trailer with a booster axle. **Figure 4** shows photographs of the combination. **Figure 5** and **Figure 6** show the articulated booster axle. The large and heavy loads transported by this tractor-trailer combination often require an articulated rear booster axle. The booster axle is attached to the trailer with

Figure 4
Truck-tractor and semi-trailer with booster axle.

Figure 5
Trailer with booster axle.

a pin and can articulate as necessary to navigate turns.

The overall length of the truck and trailer combination was 84 feet. The driver dropped off a large crane earlier in the day and was returning to the equipment yard on a road that had been driven many times prior by this rig.

Pickup Truck

The second vehicle was a 2008 four-door extended cab 4x2 pickup truck. The curb weight was 4,794 lb. The pickup was powered by a 4.7-liter V8 gasoline engine. It was equipped with an airbag control module (ACM) that stores crash data during an impact. Data was downloaded and analyzed showing that the speed at impact was 28 mph. The delta-v recorded by the pickup's ACM was 14.2 mph. The pickup truck was towing an open trailer with landscape equipment. The two occupants in the front seats of the pickup were both seriously injured in the crash.

Passenger Car

The third vehicle was a 2005 passenger car, which collided with the rear of the trailer being pulled by the pickup. This impact did not cause or contribute to the initial collision between the truck and the pickup. Since there was no substantive effect of this collision, the car's involvement will not be included in this discussion.

Analytical Method

The forensic engineering evaluation of the pre-collision events utilized custom mathematical, Computer

Figure 6
Trailer with booster axle.

Aided Drawing and Design (CADD), and physical models. The graphical, geometric, and analytical methods that were applied in the analysis included the following:

1. Created 3D CADD models based on the photographs, measurements, and laser scans of the truck and trailer to evaluate its shape and geometry in three dimensions.

2. Created 3D CADD models of the site based on measurements, total station survey data, laser scans, and mapping with aerial photos.

3. Determined tire positions of truck and trailer on the road along the travel path.

4. Determined the topography of the road surface

along the paths of the tractor and trailer tires.

5. Identified gaps between road surface and tire contact patches assuming no suspension droop. (See definition at end of section.)

6. Measured vertical loads at the contact point of trailer tires at different elevations of the tractor and booster wheels to measure suspension droop of trailer wheels, and to quantify unloading due to bridging effect of the road surface and vehicle geometries.

7. Created a detailed kinematic model of the truck-trailer configuration to determine the dynamic relationship between speed and friction for the subject trailer on the subject road.

8. Measured roadway friction with a truck tire test apparatus under wet and dry conditions. (See note at end of section.)

9. Determined speed at which trailer inertial force exceeded available traction force, causing trailer rotation.

Definition: The "gap" for the purpose of this document is the height difference between a datum established by the elevation of the booster and tractor tires on either end and the trailer tires in between.

Note: The truck tire test apparatus was a purpose-built mobile drag sled utilizing truck tires comparable to the tires on the subject trailer and was used to measure the roadway drag factor at the site and other similar roadway surfaces in the area. It was modeled after the device described in SAE J2505[2].

Evaluation of Topographic Factors

The changing roadway radius curve, the changing downhill slope, and the changing superelevation of the roadway had to be modeled accurately to determine the trailer and booster axle tire loading at specific locations along the ramp. The combined length of the truck, trailer, and booster axle created a bridge, lifting the trailer tires as the truck entered the bowl created by the exit ramp geometry. This bridging effect was exacerbated by a depression in the roadway surface at the beginning of the curve. This depression was due, in part, to the compound effect of the combined curves, as well as years of high traffic volumes and multiple maintenance and resurfacing operations.

As the trailer's weight was transferred to the articulated booster axle, the axle steered forward rather than following the curve of the exit ramp. The wet roadway enabled a loss of lateral traction at the trailer tires without complete lift or separation of the tires from the roadway.

Trailer Weighing

Wheel load measurements were conducted to study the effect of the roadway geometry on the loading of trailer axles and tires. To mimic the gap caused by the roadway geometry and trailer length, the complete rig (including tractor, trailer, and booster axle) was configured as it was on the day of the accident.

In order to quantify the wheel loading and weight transfer from axle to axle for the truck, trailer, and booster axle, the weights of each wheel load were measured on level ground and under a series of progressively increasing differential tractor/booster heights.

Scale platforms were placed under each pair of trailer and booster axle wheels on one side. Wheels on the other side and tractor wheels were supported by wood shims such that all the wheels were at the same level. The tractor and the booster wheels were lifted in ½-inch increments from an initial height of 1 inch up to a maximum of 4 inches. At each level, the loads on the trailer and booster wheels were measured with the scales and all data recorded. **Figure 7** shows the setup for the wheel load measurements.

The results showed that as the trailer gap increased, the loads on the trailer axles generally decreased —

Figure 7
Wheel load measurement.

and the load on the booster axle increased. **Figure 8** shows the wheel load of the trailer and booster axles as a function of raised height of the tractor-booster axle datum. Data from these measurements were used in the kinematic model for trailer slide-out.

Next the truck, trailer, and booster axle geometries were matched to a detailed model of the actual roadway geometry. **Figure 9** demonstrates the trailer wheel lift and gap analysis along the roadway in the area leading up to the collision event. The graph illustrates the difference in height between the asphalt and each of the trailer wheels, driver (D) and passenger (P), for each of the three axles (T1, T2, T3). The figure illustrates the tractor-trailer position when the trailer tires are in the area of maximum height difference and maximum horizontal curvature. This position correlates with the likely loss of traction and subsequent impact. Note that this analysis assumes no droop in the trailer suspension.

Figure 8
Wheel load as a function of raised height of tractor-booster axle datum.

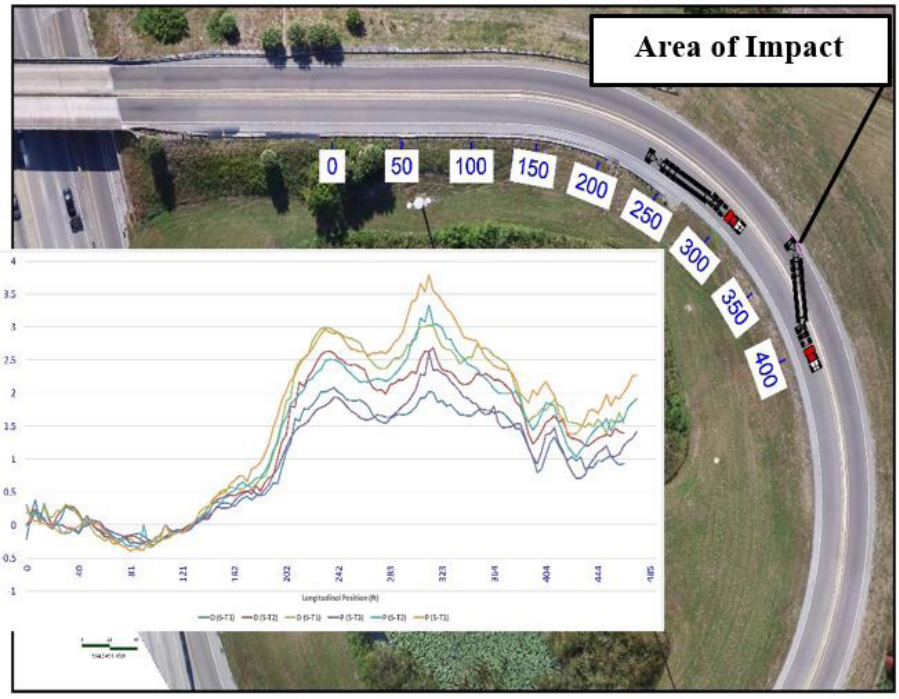

Figure 9
Elevation difference of trailer tires above roadway surface from the tractor-booster axle.

Figure 10 is a contour map of the road surface elevation and shows the tractor-trailer positions at the beginning of the wheel height difference and at the maximum height difference. **Figure 11** is a graphic representation of the trailer tire lift. **Figure 12** illustrates the bridging created by the idealized lift of the trailer due to booster axle loading. This illustration does not include suspension droop. In real-world conditions, the tires were significantly unloaded but did not lose complete contact with the road surface. Reduced normal force caused a reduction in lateral traction, which allowed the trailer to swing to the left in the right-hand curve.

The roadway surface was not significantly deteriorated. However, multiple overlays and repaving had occurred, and the center raised median was no longer functional to impede cross-over events due to the accumulation of asphalt that resulted in the increase in road surface height, as illustrated in **Figure 13**.

The vertical and horizontal components of the ramp slope and

curvature, along with the superelevation of the road surface combined to create a geometry conducive to unloading the trailer wheels for this tractor trailer. This relationship between slope and superelevation is shown in **Figure 14**.

Kinematic Model

The loss of lateral traction of the trailer tires, which permitted the booster axle to redirect the trailer into the opposing lane, was related to roadway friction, vertical loads, and location-specific roadway geometry. The configuration of this rig and the sensitivity of the wheel loading required a kinematic model specific to the facts of this event to evaluate the movement and rotational characteristics of the truck, trailer, and booster axle on this segment of roadway.

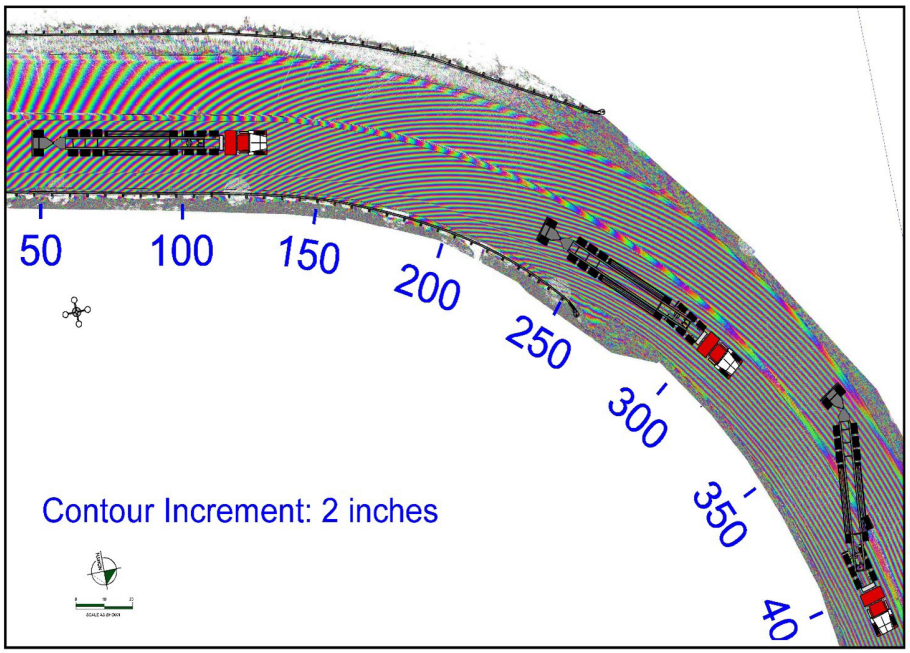

Figure 10
Truck semi-trailer position at wheel lift on road surface showing lines of constant elevation.

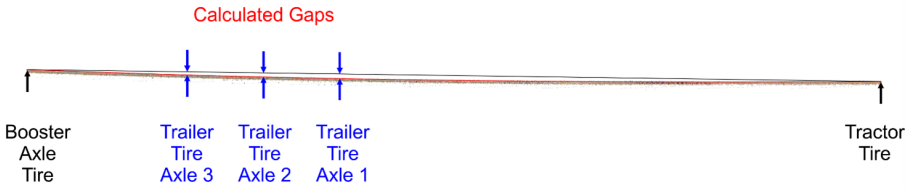

Figure 11
Gap analysis at area with loss of trailer tire friction.

Figure 12
Trailer wheel lift with booster axle loading before suspension droop.

Traditional methods to determine the critical speed of a vehicle on a curve require certain assumptions that were not applicable in this case due to the unusual geometry of this tractor trailer and the geometric configuration of the roadway[3]. Therefore, a kinematic model was created to determine the conditions necessary for the trailer to slide out during movement along this curved path by assuming that the moment about the kingpin created by the centrifugal force must exceed the resistance moment caused by the lateral friction forces of the trailer tires.

The center of mass of the trailer relative to the kingpin was calculated based on detailed measurements of the trailer using the 3D laser scan. The weights of the individual trailer components were determined through either direct measurements or from spec sheets. The center of mass of the trailer was calculated.

$$X_{cm} = \frac{1}{W_T}\sum W_i \bar{X}_i$$

Where X_{cm} is the center of mass of the trailer relative to the kingpin, W_T is the total weight of the trailer, W_i and X_i are respectively weight and relative center of mass location of individual trailer components.

The trailer wheel loads were determined based on direct measurements of individual tire loads. The resistance moment at the kingpin was calculated based on measured coefficient of friction of the wet road, trailer tire loading forces, and the moment arms from individual axles to the kingpin.

$$M_f = \sum \mu f_i X_i$$

Where M_f is the resistance

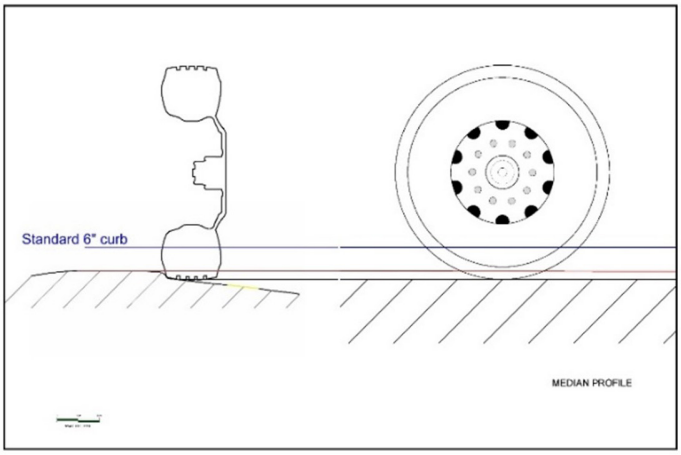

Figure 13
Center median height above road surface.

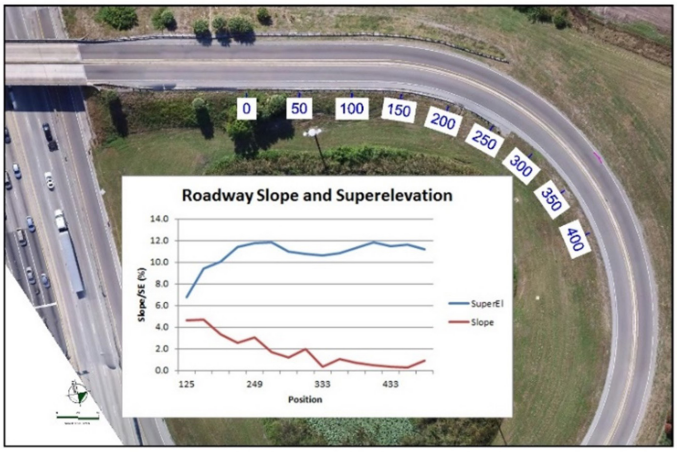

Figure 14
Superelevation road surface geometry.

moment, μ is wet road coefficient of friction that includes any roadway slope such as grade and superelevation, f_i are tire loading forces, and X_i are moment arms from individual axles to the kingpin.

The moment about the kingpin created by the centrifugal force was calculated based on the travel speed of the truck, radius of the curve, and the distance between the kingpin and the center of mass of the trailer.

$$M_C = \frac{W_T v^2}{rg} X_{cm}$$

Where M_C is the moment due to centrifugal force, v is the travel speed of the truck, r is the radius of the curve, X_{cm} is the center of mass of the trailer relative to the kingpin, and W_T is the total weight of the trailer.

When the centrifugal force moment exceeds the resistance moment the trailer will slide out. The angular acceleration of the trailer during slide-out was calculated based on equations of motion for angular momentum.

$$\sum M_{KP} = \bar{I}_{KP}\alpha$$

Where M_{KP} is the total moment about the kingpin, I_{KP} is the total moment of inertia relative to the kingpin, and α is the angular acceleration of the trailer.

The total moment of inertia relative to the kingpin was calculated using the parallel axis theorem and individual moments of inertia of the trailer components.

$$\bar{I}_{KP} = \sum[\bar{I}_i + m_i d_i^2]$$

Where I_{KP} is the total moment of inertia relative to the kingpin, I_i, m_i, and d_i respectively are moment of inertia, mass, and center of mass distances from the kingpin of individual trailer components.

The slide-out time to reach a specific slide angle at impact was calculated from angular acceleration.

$$t = \sqrt{2\theta/\alpha}$$

Where t is the slide-out time, θ is slide angle, and α is the angular acceleration of the trailer.

The maximum critical speed for the tractor-trailer at the onset of trailer slide-out as a function of roadway friction is shown in **Figure 15**. Two geometric scenarios are shown: the actual road geometry with varying slope

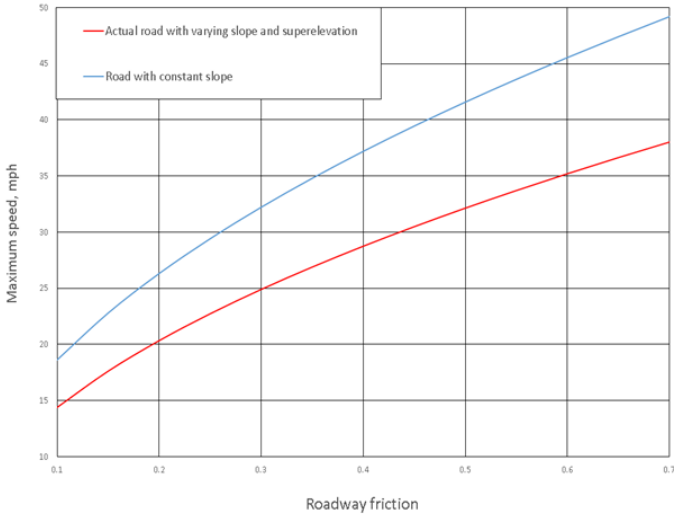

Figure 15
Maximum speed without trailer slide-out.

and superelevation, and a road with constant slope.

Conclusions

The detailed forensic engineering evaluation and reconstruction of this collision event allowed the following conclusions to be reached:

1. Changes in the roadway geometry along the path of the truck that allowed the trailer to "bridge" across lower elevation contours beginning over 250 feet before impact were quantified. The geometric characteristics were:

    a. Downslope changed from 4.5% to 1% in 142 feet (as show in **Figure 9**).

    b. Superelevation changed from 8% to 12% over 140 feet.

    c. Radius of curve continually decreased from a straight section of road to a curve with a radius of 230 feet.

2. The geometric characteristics, in combination with the long wheelbase of the trailer with booster axle, raised the height of the trailer relative to the roadway, thereby reducing the vertical load on the trailer wheels and the associated traction available to the tires needed to maintain lateral stability.

3. Rainwater acted as a lubricant to reduce the friction between the tires and the roadway. The wet friction value for a truck tire on this road surface was measured to be 0.35 (0.30 to 0.40, +/- one standard deviation). When dry, the friction value was 0.76 (0.68 to 0.85, +/- one standard deviation).

4. At the location where the trailer tires had less friction force available because of the dip and curve in the road, the curvature of the roadway created centrifugal force on the trailer. Typically, centrifugal force is resisted by the lateral traction of the tires. However, in this case, the moment about the kingpin created by the centrifugal force exceeded the lateral traction at the trailer tires at a speed of 27 mph, whereas the advisory speed was 35 mph.

5. The rotation of the trailer was caused by the combination of road surface geometry that created a bend and dip at the onset of the decreasing radius curve; the wet pavement; and the long wheelbase of the trailer with booster axle.

6. At the measured tire friction of 0.35 for the wet road, the geometry of the road surface and the geometry of this particular trailer reduced the safe travel speed for this tractor trailer from 35 to 27 mph.

As is often the case, this traffic accident arose from a combination of roadway, vehicle, operational, and environmental factors. The roadway was not in compliance with current AASHTO standards due to its age and resurfacing activities over the years — and was scheduled to be rebuilt. The tractor trailer was operated unloaded with a booster axle that interacted with the road surface to lift the trailer wheels as it passed over the wet roadway. Although the driver had reduced his speed, it was still too fast for this rig on this section of roadway when wet.

The forensic engineering analysis identified the influence of these factors on the reduction of lateral traction as a function of vehicle speed. The conclusion reached from this analysis was that, at the time of the accident, the safe travel speed for this tractor trailer was reduced from 35 mph to 27 mph, a speed below the posted advisory speed and that was consistent with the statement of the truck driver. The conclusions reached based on this detailed forensic analysis were helpful to the parties in the resolution of claims arising from this unfortunate traffic accident.

References

1. A Policy on Geometric Design of Highways & Streets AASHTO, 6th Edition, 2011.

2. Measurement of Vehicle-Roadway Frictional Drag, SAE J2505, 2010.

3. Use of the Critical Speed Formula, SAE J2969, International, Society of Automotive Engineers, Jan 2017.